Bound-Preserving Reconstruction of Tensor Quantities for Remap in ALE Fluid Dynamics

Matej Klima, Milan Kucharik, Mikhail Shashkov and Jan Velechovsky

Abstract We analyze several new and existing approaches for limiting tensor quantities in the context of deviatoric stress remapping in an ALE numerical simulation of elastic flow. Remapping and limiting of the tensor component-by-component are shown to violate radial symmetry of derived variables such as elastic energy or force. Therefore, we have extended the symmetry-preserving Vector Image Polygon algorithm, originally designed for limiting vector variables. This limiter constrains the vector (in our case a vector of independent tensor components) within the convex hull formed by the vectors from surrounding cells—an equivalent of the discrete maximum principle in scalar variables. We compare this method with a limiter designed specifically for deviatoric stress limiting which aims to constrain the J_2 invariant that is proportional to the specific elastic energy and scale the tensor accordingly. We also propose a method which involves remapping and limiting the J_2 invariant

M. Klima (✉) · M. Kucharik
Faculty of Nuclear Sciences and Physical Engineering,
Department of Physical Electronics, Czech Technical University in Prague,
Brehova 7, 115 19 Praha, Czech Republic
e-mail: klimamat@fjfi.cvut.cz

M. Kucharik
e-mail: kucharik@newton.fjfi.cvut.cz

M. Shashkov
Los Alamos National Laboratory, XCP-4 Group, MS-F644, P.O. Box 1663,
Los Alamos, NM 87545, USA
e-mail: shashkov@lanl.gov

J. Velechovsky
Los Alamos National Laboratory, T-3 Group, MS-B216, P.O. Box 1663,
Los Alamos, NM 87545, USA
e-mail: jan@lanl.gov

C. Klingenberg and M. Westdickenberg (eds.), *Theory, Numerics and Applications of Hyperbolic Problems II*, Springer Proceedings in Mathematics & Statistics 237, https://doi.org/10.1007/978-3-319-91548-7_11

independently using known scalar techniques. The deviatoric stress tensor is then scaled to match this remapped invariant, which guarantees conservation in terms of elastic energy.

Keywords ALE · Remapping · Limiter · Stress tensor · Symmetry preservation

MSC2010: 65D05 · 65M99 · 74B05

1 Introduction

The reconstruction of material quantities from discrete values defined on a computational mesh is a key part of high-order numerical schemes for fluid dynamics. For demanding simulations where both high-pressure gradients and shear flows occur simultaneously, such as in the field of laser–plasma interactions, the Arbitrary Lagrangian–Eulerian (ALE) framework [3, 6] is often used. As its name suggests, it allows for arbitrary movement of the computational mesh. We focus on the indirect ALE formulation which utilizes pure Lagrangian steps [2] advancing the solution and mesh in time.

If needed, mesh smoothing and subsequent quantity remapping are performed to preserve sufficient geometric quality of the mesh. In the remapping step, the monotonicity of the reconstructed fields is often ensured by slope limiters. These have been formulated originally for scalar and later extended to vector quantities. However, reconstructing and limiting of tensor variables are still a relatively unexplored territory with only a few specialized methods that have been proposed recently [11]. The design principles of such methods are objectivity (frame invariance) and preservation of bounds and tensor invariants.

The simplest approach presented in this paper involves piecewise linear reconstruction of the tensor components using a known limiter scheme for scalar variables (such as the Barth–Jespersen limiter [1]) applied component-wise. This method is known to violate the solution symmetry for radially symmetric problems. Our alternative scheme is inspired by the Vector Image Polygon limiter [5], constraining the tensor components within a convex hull constructed in the tensor component space.

Another approach was proposed specifically for stress tensor limiting [11], constraining its second invariant, and scaling the tensor in a way that is frame invariant and preserves local extrema and symmetry. We propose an extension of this method, based on limiting/remapping the tensor components and the J_2 invariant separately. The remapped tensor is then scaled to match the remapped J_2 value—as it is proportional to the elastic energy density, which implies that the conservation of energy will not be violated.

Properties of the particular methods are demonstrated on a selected numerical test of static remapping of a tensor quantity with a radially symmetric distribution.

2 Governing Equations—the Lagrangian Step

We solve the time-dependent Euler equations in Lagrangian form, extended to a general elastic–plastic continuum [10, 13]:

$$\rho \frac{dv}{dt} - \nabla \cdot \mathbf{u} = 0, \tag{1}$$

$$\rho \frac{d\mathbf{u}}{dt} - \nabla \cdot \sigma = 0, \tag{2}$$

$$\rho \frac{dE}{dt} - \nabla \cdot (\sigma \mathbf{u}) = 0, \tag{3}$$

where ρ represents density, $v = \frac{1}{\rho}$ specific volume, σ the Cauchy stress tensor, $\mathbf{u}$ velocity vector, and $E = \varepsilon + \frac{1}{2}\mathbf{u}^2$ specific total energy with ε being the specific internal energy. The Cauchy stress tensor is symmetric and can be decomposed as

$$\sigma = -p\,I + S, \tag{4}$$

where p is hydrodynamic pressure, I the identity matrix, and S the deviatoric stress tensor. For the closure of the system, the Mie–Gruneisen equation of state [8] is used.

The system is solved by a numerical scheme based on [10]. A compatible discretization [2] is used in which the movement of the computational mesh is calculated nodal force vectors while the discrete stress tensor is defined in cell centers. The cell-to-node subzonal forces are calculated first as

$$\mathbf{F}_{p,c} = l_1\,\sigma_c\,\mathbf{n}_1 + l_2\,\sigma_c\,\mathbf{n}_2, \tag{5}$$

and then combined to yield the total nodal force,

$$\mathbf{F}_p = \sum_{c \in N(p)} \mathbf{F}_{p,c}, \tag{6}$$

where $N(p)$ is a set containing all neighboring cells of node p. l_1, l_2 is equal to the half of the respective cell edge length, and $\mathbf{n}_1, \mathbf{n}_2$ are the unit normal vectors. See Fig. 1 for details.

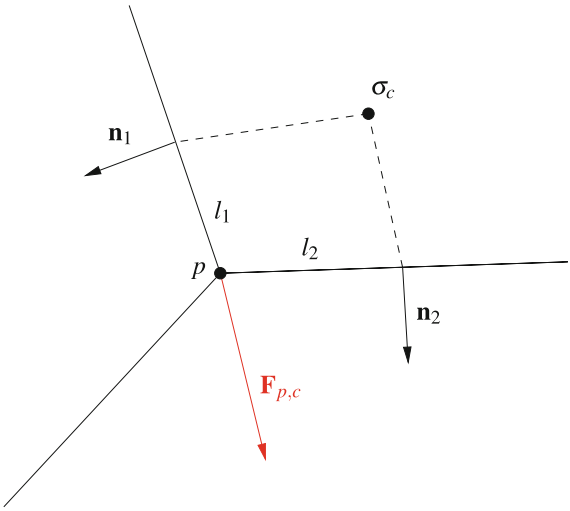

Fig. 1 Cell c to node p subzonal elastic force $\mathbf{F}_{p,c}$ construction with half-edge lengths l_1, l_2, normals $\mathbf{n}_1, \mathbf{n}_2$ and the cell-centered stress tensor σ_c

3 Remapping of the Deviatoric Stress Tensor

In this section, we propose several methods for remapping the deviatoric stress tensor. In two-dimensional planar geometry, it has the following shape:

$$S = \begin{pmatrix} S_{xx} & S_{xy} & 0 \\ S_{xy} & S_{yy} & 0 \\ 0 & 0 & -(S_{xx} + S_{yy}) \end{pmatrix}. \tag{7}$$

It is necessary to use the full 3×3 representation [10], where the third diagonal term enforces the deviatoric property $\mathrm{tr}\,(S) = 0$. The characteristic equation of the tensor defines the three invariants:

$$\lambda^3 + J_1\lambda^2 + J_2\lambda + J_3 = 0, \tag{8}$$

$$J_1 = \mathrm{tr}\,(S) = 0,\ J_2 = \frac{1}{2}(S : S) = \frac{1}{2}\mathrm{tr}(S^T S),\ J_3 = \det(S). \tag{9}$$

We are interested especially in the J_2 invariant, as it is proportional to the elastic energy density:

$$e_{\text{elast.}} = \frac{1}{2\mu} J_2, \tag{10}$$

where μ is the shear modulus, a material constant.

There are several properties, we would like the remapper to have. The first is preservation of bounds—for a tensor variable this is not readily defined but we can use one of the derived quantities. In the case of deviatoric stress, our remapper

should preserve the bounds of elastic energy [11]. The total elastic energy should also be conserved. We propose an extra criterion of preserving the elastic force radial symmetry. As a vector quantity, the elastic forces (6) are easier to analyze.

In the following subsections we describe several approaches to deviatoric stress remapping.

3.1 Component-Wise Remap and Limiting of Tensor S

The simplest way of remapping the deviatoric stress tensor is to treat the individual components of the tensor as independent scalar variables. The tensor components are remapped similarly to average pressure, where the pressure–volume work is remapped:

$$\tilde{S}^c \tilde{V}^c = S^c V^c + \sum_{c' \in \mathcal{N}(c)} \left(F^S_{c' \cap \tilde{c}} - F^S_{c \cap \tilde{c}'} \right), \quad F^S_{c' \cap \tilde{c}} = \iint_{c' \cap \tilde{c}} S(\mathbf{x}) dV. \tag{11}$$

The tensor reconstruction $S(\mathbf{x})$ can be expressed in terms of the independent tensor components as:

$$\begin{pmatrix} S_{xx} \\ S_{xy} \\ S_{yy} \end{pmatrix} (\mathbf{x}) = \begin{pmatrix} S^c_{xx} \\ S^c_{xy} \\ S^c_{yy} \end{pmatrix} + (\mathbf{x} - \mathbf{x_c}) \begin{pmatrix} \psi_{xx} \nabla S_{xx} \\ \psi_{xy} \nabla S_{xy} \\ \psi_{yy} \nabla S_{yy} \end{pmatrix}, \tag{12}$$

where ∇S is the tensor gradient and its components can be obtained using the least squares optimization [4, 7] on all neighboring cells. $\mathbf{x_c}$ is the geometric centroid of the computational cell and ψ_{xx} is a scalar limiting coefficient. In particular, the Barth–Jespersen procedure [1, 7] is used here:

$$\psi^p_{xx} = \begin{cases} \min\left(\frac{S^{\max}_{xx} - S^c_{xx}}{S^p_{xx} - S^c_{xx}}, 1.0 \right) & \text{if} \quad S^p_{xx} > S^c_{xx} \\ \min\left(\frac{S^{\min}_{xx} - S^c_{xx}}{S^p_{xx} - S^c_{xx}}, 1.0 \right) & \text{if} \quad S^p_{xx} < S^c_{xx} \\ 1.0 & \text{otherwise} \end{cases}, \tag{13}$$

$$\psi_{xx} = \min_{p \in \mathcal{P}(c)} \left(\psi^p_{xx} \right), \quad S^p_{xx} = S^c_{xx} + (\mathbf{x}_p - \mathbf{x}_c) \nabla S^c_{xx}, \tag{14}$$

where $\mathcal{P}(c)$ is the set of all vertices of the cell c, $\mathbf{x}_p$ is the position of the vertex p, and S^p_{xx} is the unlimited reconstruction in the corresponding point. $S^{\max}_{xx}$ and $S^{\min}_{xx}$ are tensor component maximum and minimum calculated on the same 9-cell stencil as is used for the gradient computation. The same procedure is also used for the other independent tensor components S_{xy} and S_{yy}.

3.2 VIP Limiter for Tensors

The component-wise limiting approach is simple to implement but it also has several disadvantages. For simplicity, let us apply this method on vectors first. Due to the independent limiting of vector components, vectors can be unnecessarily rotated, distorting the directional symmetry. In the tensor case, this can manifest as deformation of the tensor principal directions. Component-wise limiting also does not guarantee the validity of the discrete maximum principle for vector magnitudes. This is more complex for tensors, but similarly the J_2 invariant monotonicity is not preserved [11].

To solve these issues, the Vector Image Polygon limiter was proposed [5] and adapted for the vector magnitude monotonicity problem [12]. It constrains the reconstructed vector within the convex hull formed by the values in the neighboring cells. An example and comparison with the component-wise method is shown in Fig. 2—an extreme case is displayed, where all values reconstructed in vertices lie outside the convex hull in the tensor component space, but are considered valid by the component-wise limiter.

We propose applying this method as a scalar slope limiter using (S_{xx}, S_{xy}, S_{yy}) as the 3D tensor component space:

$$S(\mathbf{x}) = S^c + \psi_{VIP}(\mathbf{x} - \mathbf{x}_c)\nabla S^c, \tag{15}$$

$$\psi_{VIP} = \min_{p \in \mathscr{P}(c)} \left(\frac{\|S^{VIP} - S^c\|}{\|S^p - S^c\|} \right), \; S^p = S^c + (\mathbf{x}_p - \mathbf{x}_c)\nabla S. \tag{16}$$

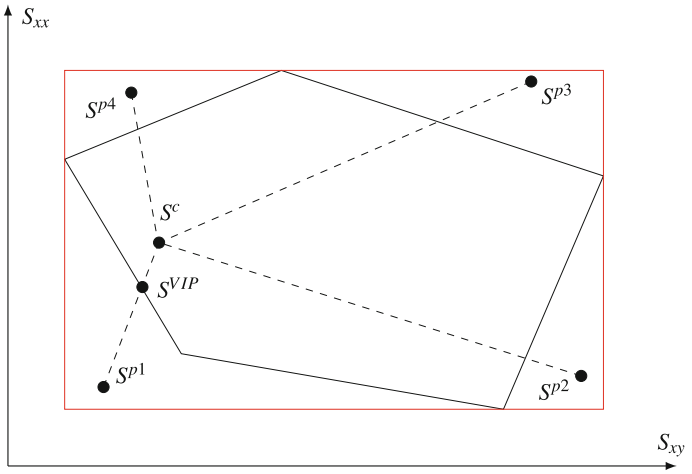

Fig. 2 A simplified 2D schematic of the VIP algorithm for tensors with unlimited reconstructed values in cell nodes $S^{p1} \ldots S^{p4}$, cell-centered average value S^c and the closest limited value S^{VIP}, compared with component-wise limiting set (red)

The construction of the convex hull in three dimensions with few points is relatively simple, but the limiter requires a robust intersection algorithm as the hull often degenerates to a planar case which needs to be treated separately. In the non-degenerate 3D case, an iterative line–polyhedron intersection is calculated.

The main disadvantages of this algorithm are complexity and more diffusion compared to component-wise limiting. It noticeably reduces the overall order of accuracy below second-order.

3.3 J_2 Invariant Scaling Limiter

This limiter was formulated specifically for the deviatoric stress limiting in [11]. It is based on an assumption that the monotonicity of J_2 invariant (proportional to elastic energy) is more important than monotonicity of tensor components. The monotonicity condition can be described as:

$$J_2^{\min} - J_2^c \leq J_2^p - J_2^c \leq J_2^{\max} - J_2^c \quad \forall p \in \mathscr{P}(c), \tag{17}$$

where $J_2^{\min}$ and $J_2^{\max}$ are again determined on the set of neighboring cells. Single scaling factor is then used for the reconstructed tensor:

$$\psi = \sqrt{\psi_{J_2} + (1 - \psi_{J_2})\frac{J_2^c}{J_2^p}}, \quad \psi_{J_2} = \textit{Barth-Jespersen}\left[J_2(S)\right], \tag{18}$$

$$S(\mathbf{x}) = \psi\left(S^c + (\mathbf{x} - \mathbf{x_c})\nabla S\right). \tag{19}$$

This approach is relatively fast, simple to implement, and the monotonicity of J_2 is guaranteed by design. However, as it has been developed in a different context, its effect on elastic forces has not been investigated in literature previously.

3.4 J_2 Invariant-Based Scalar Slope Limiter

An alternative to previous approach is also presented in [11]. The design goals are similar, but it uses the formalism of a slope limiter:

$$S(\mathbf{x}) = S^c + (\mathbf{x} - \mathbf{x_c})\psi\nabla S, \quad \psi = \textit{Barth-Jespersen}\left[\sqrt{J_2(S)}\right] \tag{20}$$

Our test show that its behavior is almost indistinguishable from the previous case while being slightly more resource intensive.

3.5 Independent Remap of S and J_2

The previously described algorithms were intended mainly to reduce symmetry distortion by using tensor-specific limiting techniques. Here we propose a different approach for deviatoric stress remapping—the J_2 invariant is remapped independently of S:

$$\tilde{J}_2^c \tilde{V}^c = J_2^c V^c + \sum_{c' \in \mathcal{N}(c)} F^{J2}_{c' \cap \tilde{c}} - F^{J2}_{c \cap \tilde{c}'}. \tag{21}$$

A scalar limiter is then used in the J_2 reconstruction. This is equivalent to remapping the elastic energy density (10) which is a conservative quantity. Then, S is remapped component-wise (11) without limiting and the resulting tensor is scaled by multiplying by the ratio of the remapped invariant $\tilde{J}_2^c$ and $J_2(\tilde{S})$ calculated from remapped S:

$$\tilde{\tilde{S}} = \tilde{S} \sqrt{\frac{\tilde{J}_2^c}{J_2(\tilde{S})}}. \tag{22}$$

This formulation guarantees conservation of total elastic energy as well as its monotonicity. The component-wise remap of S primarily determines the principal directions of the tensor (not its J_2 invariant) and according to our observation, low-order (donor) remapping is sufficient here with negligible impacts on the overall accuracy.

4 Numerical Results—Cyclic Remapping of a Nonlinear Radial Distribution of the Deviatoric Stress Tensor

We demonstrate the performance of different deviatoric stress remapping methods on a simple static test case—a distribution of the stress tensor is initialized and repeatedly remapped without any influence of the hydrodynamics. The artificial rezoning motion was inspired by the "tensor-product" cyclic rezoning [9] and is defined as follows:

$$r_n = r_l + \left[\frac{r_0 - r_l}{r_r - r_l}(1 - d_n) + \left(\frac{r_0 - r_l}{r_r - r_l} \right)^3 d_n \right] (r_r - r_l), \tag{23}$$

$$\varphi_n = \varphi_0,\ d_n = \frac{1}{2} \sin\left(\frac{\pi n}{n_{\max}} \right),\ r_l = 0.1,\ r_r = 1.0,$$

where r_0, φ_0 are the initial nodal polar coordinates, n is the current remapping step, and $n_{\max}$ is the total number of remapping steps. This represents a cyclic movement of nodes in the radial direction where the initial ($n = 0$) and final ($n = n_{\max}$) grids are identical; see Fig. 3.

On such grid, the deviatoric stress tensor is initialized as follows:

$$S_{i,j} = \begin{cases} \begin{pmatrix} 0 & 0 \\ 0 & 0 \end{pmatrix} & \text{for } i \leq \frac{n_i}{2} \\ \begin{pmatrix} -\cos(2\varphi_{i,j}) & -\sin(2\varphi_{i,j}) \\ -\sin(2\varphi_{i,j}) & \cos(2\varphi_{i,j}) \end{pmatrix} & \text{for } i > \frac{n_i}{2} \end{cases}, \tag{24}$$

where i, j are the radial and axial indices, and n_i is the number of cells in the radial direction. This distribution generates a radial discontinuity with a peak in the elastic force (as shown in Fig. 4) and piecewise constant J_2 invariant distribution.

A comparison of the final elastic force distribution after the cyclic remapping is shown in Fig. 5. If no limiter is used, there are visible undershoots of the remapped quantity. However, limiting components independently does not solve the problem and adds asymmetry. The VIP limiter performs well, but is slightly more diffusive than the other alternatives. Our approach to tensor remap seems to shift the position of the peak, but preserves monotonicity of forces perfectly in this test.

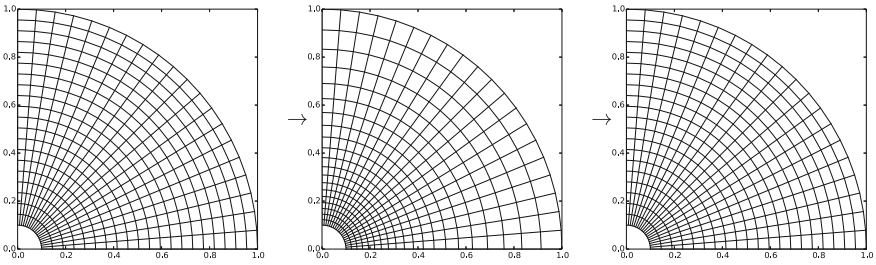

Fig. 3 Polar grid sequence—different steps of the cyclic rezoning movement, 20 × 20 mesh

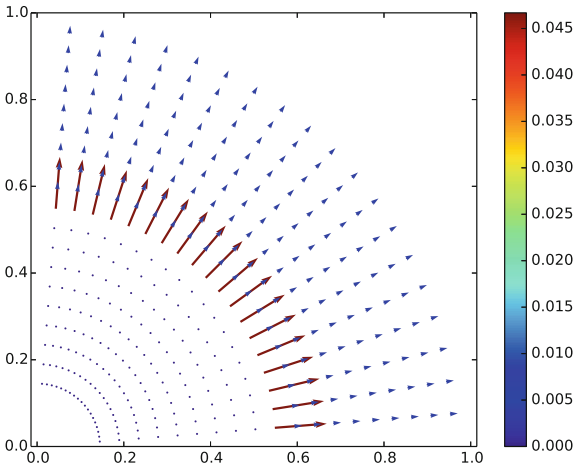

Fig. 4 Initial elastic force distribution shown in the internal nodes of the 20 × 20 mesh, force vectors are colored according to magnitude

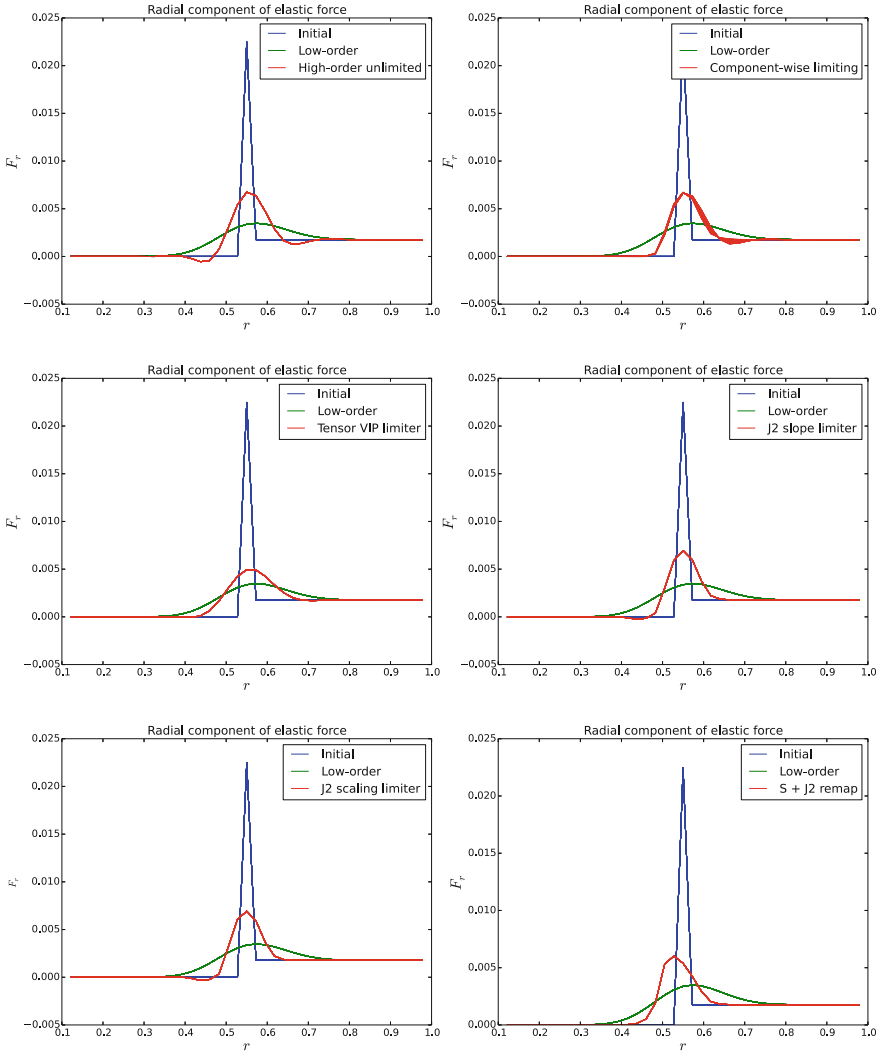

Fig. 5 Radial component of the total nodal elastic force produced by the deviatoric stress tensor after cyclic remapping, compared by different remapping methods. 40×40 mesh, $n_{\max} = 80$

Figure 6 shows the radial distribution of the J_2 invariant. Here, the asymmetry generated by component-wise limiting is even stronger. The VIP limiter does not guarantee monotonicity of the elastic energy. All other methods are based on constraining the J_2 invariant directly and therefore are successful in this task. Our remapping method preserves symmetry, does not violate energy conservation, and is the only one which limits both J_2 and elastic forces correctly in this idealized test.

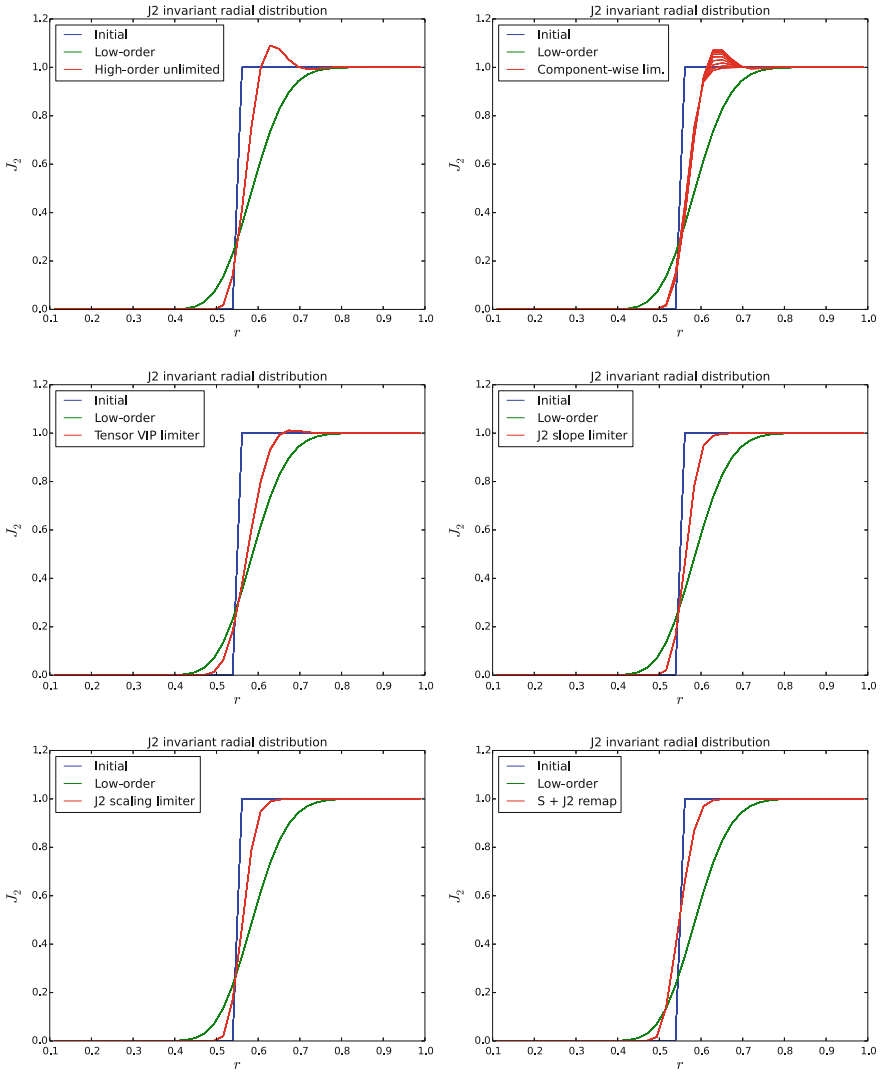

Fig. 6 Radial distribution of the J_2 invariant of the deviatoric stress tensor after cyclic remapping, compared by different remapping methods. 40×40 mesh, $n_{\max} = 80$

Table 1 illustrates the computational efficiency of all limiting methods for the cyclic remapping case. We can see that most high-order methods with limiting perform similarly, except for the VIP-based method which is much more expensive.

Table 1 Simulation times for deviatoric stress tensor cyclic remapping compared by different remapping methods, 40×40 mesh, $n_{\max} = 80$, run single-thread on an Intel^{TM} Core i5-4300M processor

Low-order	High-order unlim.	Comp.-wise lim.	VIP	J_2 scaling	J_2 slope lim.	$S + J_2$ remap
$0.3s$	$1.4s$	$1.7s$	$6.6s$	$1.7s$	$1.9s$	$1.7s$

5 Conclusion

Several methods of reconstructing a tensor quantity are proposed in this paper, focusing on the flux-form remap of the deviatoric stress in the context of an indirect ALE simulation. We show that using a scalar reconstruction method for each independent tensor component does not guarantee the monotonicity preservation of elastic forces and energy while distorting the symmetry of the solution severely.

We have implemented a modified Vector Image Polygon limiter for tensors, showing the viability of this approach. It is, however, a resource-intensive and complex method that produces more diffusive results. Specialized methods constraining the second invariant of the tensor are much faster and less diffusive but also reduce the force overshoots less.

We propose a new method for remapping the deviatoric stress, where the tensor and its second invariant are remapped independently. The tensor is then scaled to match the remapped invariant. Without much overhead, this method preserves monotonicity and guarantees the conservation of the elastic energy.

Future work includes testing the reconstruction methods in a full elastic–plastic simulations and possibly developing methods that work for general tensors.

Acknowledgements This work was performed under the auspices of the National Nuclear Security Administration of the US Department of Energy at Los Alamos National Laboratory under Contract No. DE-AC52-06NA25396 and supported by the DOE Advanced Simulation and Computing (ASC) program. The authors acknowledge the partial support of the DOE Office of Science ASCR Program. This work was partially supported by the Czech Technical University grant SGS16/247/OHK4/3T/14, the Czech Science Foundation project 14-21318S and by the Czech Ministry of Education project RVO 68407700.

References

1. T.J. Barth, Numerical methods for gasdynamic systems on unstructured meshes, in *An Introduction to Recent Developments in Theory and Numerics for Conservation Laws, Proceedings of the International School on Theory and Numerics for Conservation Laws*, ed. by C. Rohde, D. Kroner, M. Ohlberger. Lecture Notes in Computational Science and Engineering (Springer, Berlin, 1997). ISBN 3-540-65081-4
2. E.J. Caramana, D.E. Burton, M.J. Shashkov, P.P. Whalen, The construction of compatible hydrodynamics algorithms utilizing conservation of total energy. J. Comput. Phys. **146**(1), 227–262 (1998)

3. C.W. Hirt, A.A. Amsden, J.L. Cook, An arbitrary Lagrangian-Eulerian computing method for all flow speeds. J. Comput. Phys. **14**(3), 227–253 (1974)
4. M. Kucharik, *Arbitrary Lagrangian-Eulerian (ALE) Methods in Plasma Physics*. PhD thesis, Czech Technical University in Prague (2006)
5. G. Luttwak, J. Falcovitz, Slope limiting for vectors: a novel vector limiting algorithm. Int. J. Numer. Methods Fluids **65**(11–12), 1365–1375 (2011)
6. L.G. Margolin, Introduction to "An arbitrary Lagrangian-Eulerian computing method for all flow speeds". J. Comput. Phys. **135**(2), 198–202 (1997)
7. D.J. Mavriplis, Revisiting the least-squares procedure for gradient reconstruction on unstructured meshes, in *AIAA 2003–3986 2003, 16th AIAA Computational Fluid Dynamics Conference, June 23–26, Orlando, Florida* (2003)
8. R. Menikoff, Equations of state and fluid dynamics. Technical Report LA-UR-07-3989, Los Alamos National Laboratory (2007)
9. L.G. Margolin, M. Shashkov, Second-order sign-preserving remapping on general grids. Technical Report LA-UR-02-525, Los Alamos National Laboratory (2002)
10. P.-H. Maire, R. Abgrall, J. Breil, R. Loubere, B. Rebourcet, A nominally second-order cell-centered Lagrangian scheme for simulating elasticplastic flows on two-dimensional unstructured grids. J. Comput. Phys. **235**, 626–665 (2013)
11. S.K. Sambasivan, M. Shashkov, D.E. Burton, Exploration of new limiter schemes for stress tensors in Lagrangian and ALE hydrocodes. Comput. Fluids **83**, 98–114 (2013)
12. J. Velechovsky, M. Kucharik, R. Liska, M. Shashkov, Symmetry-preserving momentum remap for ALE hydrodynamics. J. Phys.: Conf. Ser. **454**, 012003 (2013). IOP Publishing
13. M.L. Wilkins, Calculation of elastic-plastic flow. Technical Report UCRL-7322, California. University Livermore. Lawrence Radiation Laboratory (1963)